Microplastics in the atmosphere of Ahvaz City, Iran

Sajjad Abbasi [1,2], Neamatollah Jaafarzadeh [3,*], Amir Zahedi [4], Maryam Ravanbakhsh [5], Somayeh Abbaszadeh [5], Andrew Turner [6]

[1] Department of Earth Sciences, College of Science, Shiraz University, Shiraz 71454, Iran

[2] Department of Radiochemistry and Environmental Chemistry, Faculty of Chemistry, Maria Curie-Skłodowska University, Lublin 20-031, Poland

[3] Environmental Technologies Research Center, Ahvaz Jundishapur University of Medical Sciences, Ahvaz, Iran

[4] Department of Environmental Health Engineering, Shoushtar Faculty of Medical Sciences, Shoushtar, Iran

[5] Student Research Committee, Ahvaz Jundishapur University of Medical Sciences, Ahvaz, Iran

[6] School of Geography, Earth and Environmental Sciences, Plymouth University, PL4 8AA, UK

Corresponding Author: Neamatollah Jaafarzadeh, email: jaafarzadeh-n@ajums.ac.ir

Accepted 6th November 2021

https://doi.org/10.1016/j.buildenv.2021.108562

Graphical Abstract

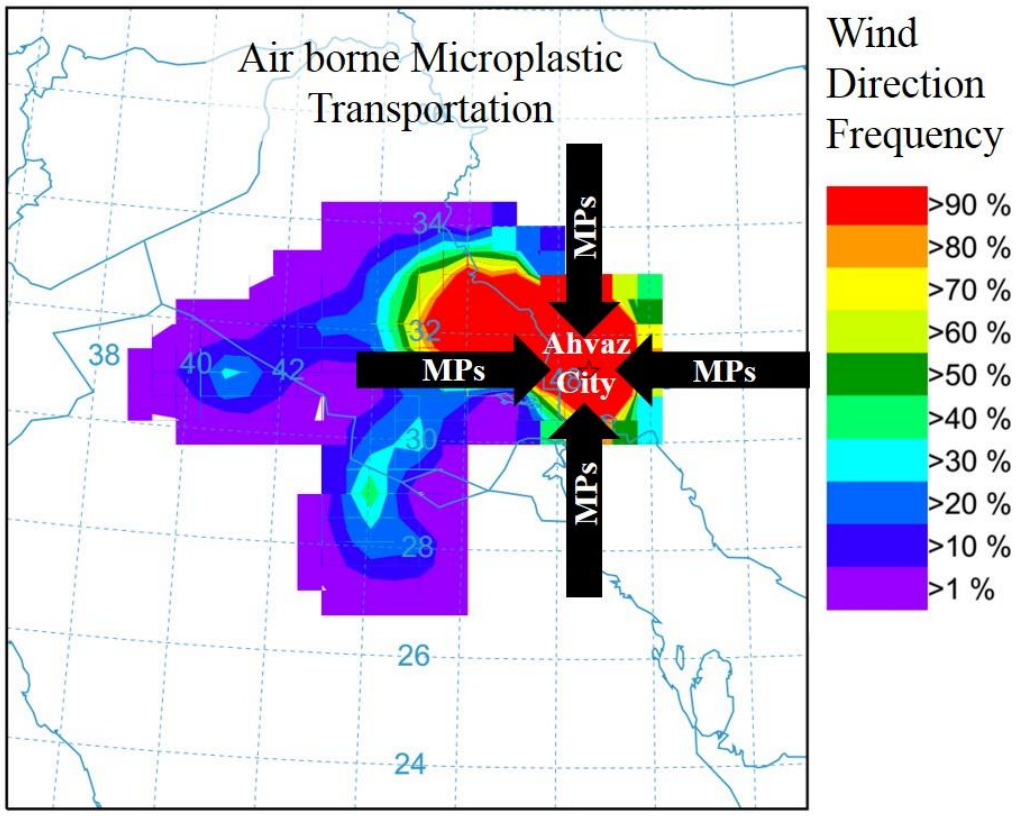

Highlights

- Airborne particulate matter was collected from urban and industrial sites in Ahvaz.
- Microplastics (MP) were isolated from samples and characterised by established techniques.
- All MP were fibrous and the dominant polymers were PET and polypropylene.

- Concentrations of MP (< 0.017 m^{-3}) exhibited no clear temporal trends or inter-site differences.
- Sample characteristics and trajectory modelling suggest both local and long-range sources.

Abstract

Airborne particulate matter (PM) with an aerodynamic size cutoff of 10 μm (PM10) has been collected using a high volume air sampler at two locations (urban and residential) in the city of Ahvaz, Iran, for sixteen 24-hour periods over four months (late summer to early winter). Microplastics (MPs) in the PM were isolated after sample digestion and were subsequently characterised by established techniques. All MPs sampled (n = 322) were of a fibrous nature, with polyethylene terephthalate and polypropylene being the dominant polymers and consistent with textiles and fabrics as the principal source. Despite a distinct seasonality (temperature and wind) over the study period, the abundance, size and colour of the fibres exhibited no clear temporal trend, and no clear differences were observed between the two sites. Concentrations of MPs ranged from none detected to about 0.017 per m^3 (median = 0.0065 m^{-3}) and are at the low end of ranges reported in the recent literature for various urban and remote locations. While some MPs may have a local origin, the weathering of other MPs and their acquisition of extraneous geosolids and salts suggests that long-range transport is also important. Back-trajectory calculations indicate that regional sources are mainly to the north and west of Ahvaz, but a southerly, maritime source is also possible in late autumn. Although concentrations of MPs in the atmosphere are well below those encountered in indoor air, further studies are required to elucidate their potential ecological impacts.

Keywords: microplastics; atmosphere; transport; fibres; polymers; Ahvaz

1. Introduction

Microplastics (MPs) are pervasive and ubiquitous environmental contaminants that have received intensive scientific study over the past two decades (Browne et al., 2011; Li et al., 2018; Buks and Kaupenjohann, 2020). Amongst the environmental compartments, the atmosphere has gained the least attention in this respect, despite being an important receptor and transporter of pollutants more generally (Zhang et al., 2020). A variety of polymers and forms or shapes of MP exist in the atmosphere but the particle population appears to be dominated by fibres that are derived from clothing, decorative, automotive, agro-, medical and industrial textiles and fabrics (Cai et al., 2017; Allen et al., 2019; Roblin et al., 2020; Wright et al., 2020). Plastic-based fibres generally co-exist with fibres derived from other artificial and natural (but processed) substances that have similar aerodynamic properties (Dris et al., 2016; Dris et al., 2017; Liu et al., 2019a; Stanton et al., 2019; Constant et al., 2020).

Both passive and active sampling approaches have revealed that MPs widely exist in the atmosphere and undergo dry and wet deposition, with their detection in areas remote from population centres, industrial activities or agricultural practices indicating a propensity for long-range transport (~ 1000 km) with air-masses (Bergmann et al., 2019; Brahney et al., 2020). Long-range transport acts as a vector for the direct input of airborne MPs into the oceans (Liu et al., 2019b; Szewc et al., 2021) but evidence also suggests oceans may act as an indirect source of MP to the atmosphere through bubble burst ejection and wave action (Allen et al., 2020).

In order to better our understanding of the nature and behaviour of MPs in the atmosphere, we used a high volume air sampler to collect material from the lower atmosphere of an urban arid environment (Ahvaz, Iran). Specifically, we employed a standardised EPA method for the collection of particulate matter (PM10) on sixteen occasions over a four-month period from an

urban and industrial location. MPs were determined after sample digestion in H_2O_2 and particle separation by density and were subsequently characterised according to shape-form, size and polymeric construction using established techniques. This information, coupled with back trajectory calculations, was used to gain an insight into the sources, environmental drivers and potential health impacts of airborne MP in the region.

2. Material and Methods

2.1. Study area

The city of Ahvaz lies on the Karun River on the Khuzestan plain (at about 20 m above sea level) in southwest Iran. Ahvaz is an important economic and industrial centre and, with a population of about 1,300,000, is the largest city and capital of Khuzestan province. The city experiences a subtropical hot desert climate, with long hot summers (when temperatures can exceed 50 ^{o}C and dust storms and sand storms occur) and cool short winters (when temperatures can be as low as 5 ^{o}C). Annual average rainfall is about 230 mm and prevailing winds are from the northwest.

2.2. Sampling of air-borne particulate matter

A total of 32 suspended particulate matter (PM) samples were collected from two locations on 16 occasions free from any precipitation and at 7- to 11-day intervals between summer and winter, 2019. Station 1 (S1; industrial) is to the east of the Karun River and is close to a steel factory, landfill site and carbon black and pipe manufacturers and has a relatively low traffic load; station 2 (S2; urban) is to the west of the river and is located in a more residential and light industrial setting but has a relatively high traffic load (Figure 1).

112 Samples of PM were collected on pre-weighed, 203 x 254 mm rectangular glass-fibre filters
113 (1.6 µm pore size; Whatman G653) using a Tisch high volume air sampler. Here, air is drawn
114 through a size-selective sampling inlet and the filter medium by means of a blower, with
115 particles whose aerodynamic diameters are less than the cut-point of the inlet collected on the
116 filter. We selected a size cutoff of 10 µm (PM10) and, in accordance with US EPA references
117 methods (EPA, 1999), deployed the sampler at a height of 10 m above ground level and with
118 a flow rate of 1.3 m^3 per minute. After 24 h, filters were transferred to glass petri dishes that
119 had been washed with filtered (2 µm), deionised water before being returned to the laboratory
120 for MP extraction and counting.

121

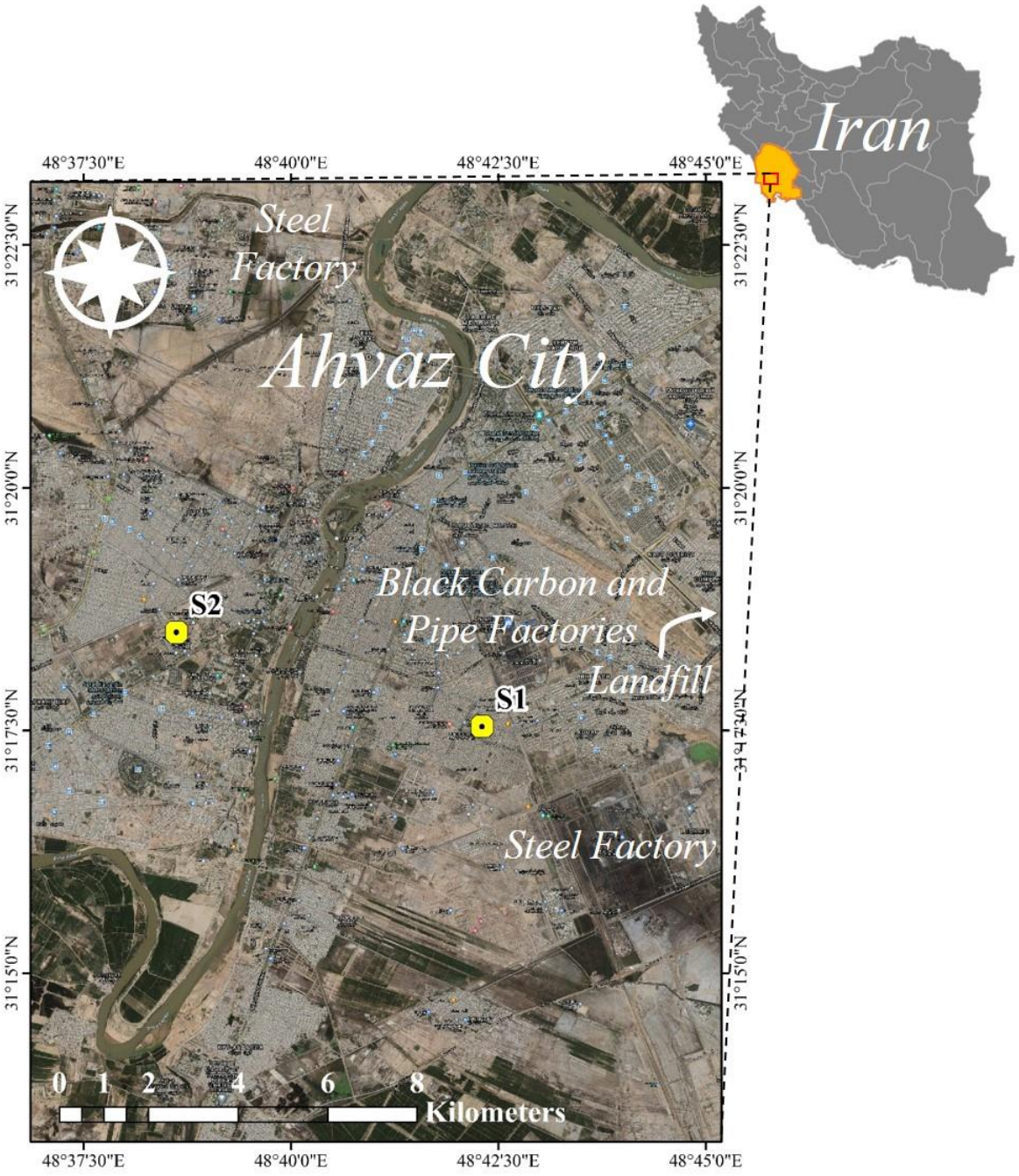

122

123 Figure 1. Suspended particulate matter sampling stations in the city of Ahvaz, Iran

124

125 *2.3. Extraction and counting of microplastics*

126 Filters were stored in a desiccator at 25 °C and for 24 h before being weighed using an
127 electronic analytical microbalance (LIBROR AEL-40SM, Shimadzu). Each filter was then

placed in a glass beaker with filtered, deionized water and the contents shaken for 24 h at 350 rpm. Any visible material remaining on the filter was carefully dislodged with a metallic razor and the particle-water suspension subsequently transferred to a clean beaker that was then placed in a sand bath at 80 ^{o}C. Before the water had completely dried, residues were mixed with 35 mL of 30% H_2O_2 (Arman Sina, Tehran) for 10 d at room temperature in order to remove organic matter. Residual particulate material was then retrieved by vacuum-filtering the remaining H_2O_2 solution through an S&S filter paper (2 µm pore size). Fifty mL of a saturated solution of $ZnCl_2$ (Arman Sina, Tehran) and a density of 1.6 to 1.8 g cm^3 was added to each filter in a clean beaker and the contents shaken for 5 min at 350 rpm before being allowed to settle for 1 h. The overlying liquid was carefully siphoned off and centrifuged for 3 min at 4000 rpm and the supernatant vacuum-filtered onto a new S&S filter. To capture all MPs, the process of density separation, centrifuging and filtering was repeated twice through the same filter. Filters were dried in a metal cabinet at room temperature for a few days before being transferred to individual glass Petri dishes for counting.

For the identification of MPs and the exclusion of other materials (including rubbers) derived from the airborne PM samples, binocular microscopy (Carl-Zeiss) was used with commonly employed visual characteristics (e.g. form, opacity, hardness, gloss) and reaction to a hot stainless steel probe (Hidalgo-Ruz et al., 2012; Abbasi et al., 2019). MPs were classified according to colour as white-transparent, yellow-orange, red-pink, blue-green or black-grey, according to shape as fibre, film, fragment or spherule, and, with the aid of the probe and ImageJ software, according to length or primary diameter, L ($L \leq 100$ µm; $100 < L \leq 250$ µm; $250 < L \leq 500$ µm; $500 < L \leq 1000$ µm; $L > 1000$ µm). Based on the optical microscopy results, the topography and elemental composition of selected MP ($n = 24$) recovered from the PM samples were determined through high vacuum scanning electron microscopy/energy-dispersive X-ray microanalysis (SEM/EDX) using a Tescan VEGA 3 microscope (with a

153 resolution of 2 nm at 20 kV) and an Oxford Instruments X-Max 50 silicon drift detector with
154 AZtec and INCA software. Here, samples that had been carefully brushed from the filters were
155 mounted on double-sided adhesive carbon tabs on aluminium SEM stubs. The polymeric
156 construction of 19 MP of a range of shapes, sizes and colours was determined using a micro-
157 Raman spectrometer (LabRAM HR, Horiba, Japan) with a laser of 785 nm and Raman shift of
158 400-1800 cm^{-1} and with acquisition times between 20 and 30 s.

159

160 *2.4. Quality control*

161 In order to prevent plastic contamination during the extraction phase of the air-borne PM
162 samples in the laboratory, all reagents and distilled water were filtered through S&S blue band
163 filters, working surfaces were thoroughly wiped with ethanol, all glassware was cleaned with
164 distilled water and all windows and doors were closed. White cotton laboratory coats, single-
165 use latex gloves and facemasks were worn throughout sample manipulation and processing
166 and, where possible, samples and containers were protected by aluminium foil. Two beakers
167 containing filtered water only were subject to the same procedures as beakers that originally
168 contained sample (glass fibre) filters and filtered water. Analysis of final (S&S) filters arising
169 from this process revealed no detectable MP contamination under the working conditions
170 employed. For replication purposes, three random filters from both stations were recounted for
171 MPs, with results being identical in each case.

172

173 *2.5. Trajectory modelling*

174 The potential source range of MP to the study area was determined from back trajectory
175 frequencies calculated using the National Oceanic and Atmospheric Administration online
176 software, Hybrid Single Particle Lagrangian Integrated Trajectory (HYSPLIT), and Global

Forecast System (0.25 degree global) meteorological data. Thus, on each sampling occasion, 24-hour backward trajectories were computed from Ahvaz at eight-hour intervals and for the 48-h preceding sampling at a height of 500 m above ground level and a resolution of 1 degree. Integrated trajectory data were then used to plot percentage frequency distributions. This approach is commonly used to infer airborne MP sources (Brahney et al., 2020; González-Pleiter et al., 2021), although the model itself does not account for particulate transport or particle deposition unless appropriate parameters are included.

3. Results

The mass concentrations of PM (with a maximum aerodynamic diameter of 10 μm and per m^3 of air) are shown in Table 1 for both stations and on each occasion sampled. Mean, minimum and maximum concentrations are similar at S1 (68.46, 35.34 and 98.34 μg m^{-3}, respectively) and S2 (63.62, 39.64 and 94.64 μg m^{-3}, respectively) and, overall, there was relatively little variation amongst the measurements (relative standard deviation ~ 25%; n = 32). Moreover, there was no clear relationship between PM concentration and date, mean air temperature or mean wind speed for either station and no significant (linear) relationship ($p > 0.05$) between concentrations at the different sites determined on the same dates.

The number of MPs recovered from each filter deployed for a 24-h period was more variable, ranging from none detected (on five occasions) to 31 at S1 and none detected (on two occasions) to 28 at S2. Where MPs were detected, concentrations on a number basis ranged from about 0.002 to 0.017 m^{-3} and from 23 to 341 per g of PM at S1 and about 0.002 to 0.015 m^{-3} and from 34 to 162 per g of PM at S2, with no significant differences ($p > 0.05$ according to Kruskal-Wallis tests) in the means of either measure between the two stations.

Table 1: Mean daily air temperatures and wind speeds, and concentrations of PM and the number and concentrations of MPs (per m^3 of air and per g of PM) at stations S1 and S2 determined over sixteen 24-h periods in 2019 (nd = none detected).

			S1				S2			
Date	Temp., °C	Wind speed, km h^{-1}	[PM], µg m^{-3}	MP, *n*	[MP], *n* m^{-3}	[MP], *n* g^{-1}	[PM], µg m^{-3}	MP, *n*	[MP], *n* m^{-3}	[MP], *n* g^{-1}
28/08/2019	40	6.4	74.59	13	0.0069	93	42.36	8	0.0043	101
04/09/2019	39	30.5	66.34	15	0.0080	121	86.29	20	0.0107	124
15/09/2019	37	12.9	57.61	17	0.0091	158	51.39	12	0.0064	125
22/09/2019	33	8.0	48.57	31	0.0166	341	62.46	16	0.0085	137
29/09/2019	33	20.9	94.67	13	0.0069	73	53.67	8	0.0043	80
06/10/2019	30	11.3	98.34	12	0.0064	65	72.64	16	0.0085	118
31/10/2019	28	12.9	78.64	nd	nd	nd	53.64	9	0.0048	90
20/09/2019	25	17.7	72.38	9	0.0048	66	57.67	16	0.0085	148
28/10/2019	20	12.9	94.67	4	0.0021	23	83.64	12	0.0064	77
06/11/2019	20	11.3	67.69	nd	nd	nd	39.64	5	0.0027	67
31/11/2019	20	11.3	61.67	nd	nd	nd	47.59	3	0.0016	34
21/11/2019	18	6.4	35.34	9	0.0048	136	51.67	13	0.0069	134
29/11/2019	16	8.0	67.12	8	0.0043	64	55.84	nd	nd	nd
07/12/2019	16	22.5	54.63	nd	nd	nd	94.64	16	0.0085	90
14/12/2019	16	9.6	65.59	nd	nd	nd	92.46	28	0.0150	162
22/12/2019	15	4.8	57.48	9	0.0048	84	72.34	nd	nd	nd

In total, 322 MPs were identified amongst the PM samples, with binocular microscopy indicating that all particles were of a fibrous nature. The sizes and colours of the MPs are summarised in Figure 2 for both stations. Thus, at S1, each size range comprised about 20-30% of the particle population with the exception of 500 to 1000 µm (about 5%), while at S2 all size ranges contributed roughly equally to the population. Note that the MPs identified by microscopy were larger than the inlet size of the air sampler (PM10) reflecting aerodynamic properties of MPs that are very different to those of dust particulates. Regarding colour, black-grey was dominant (about 60% and 70% of MP at S1 and S2, respectively), with percentage contributions from remaining colours < 20 and yellow-orange fibres entirely absent. Analysis of 19 MPs by Raman spectrometry revealed that nine were constructed of polyethylene terephthalate (PET), five were polypropylene, three were nylon and two were polystyrene.

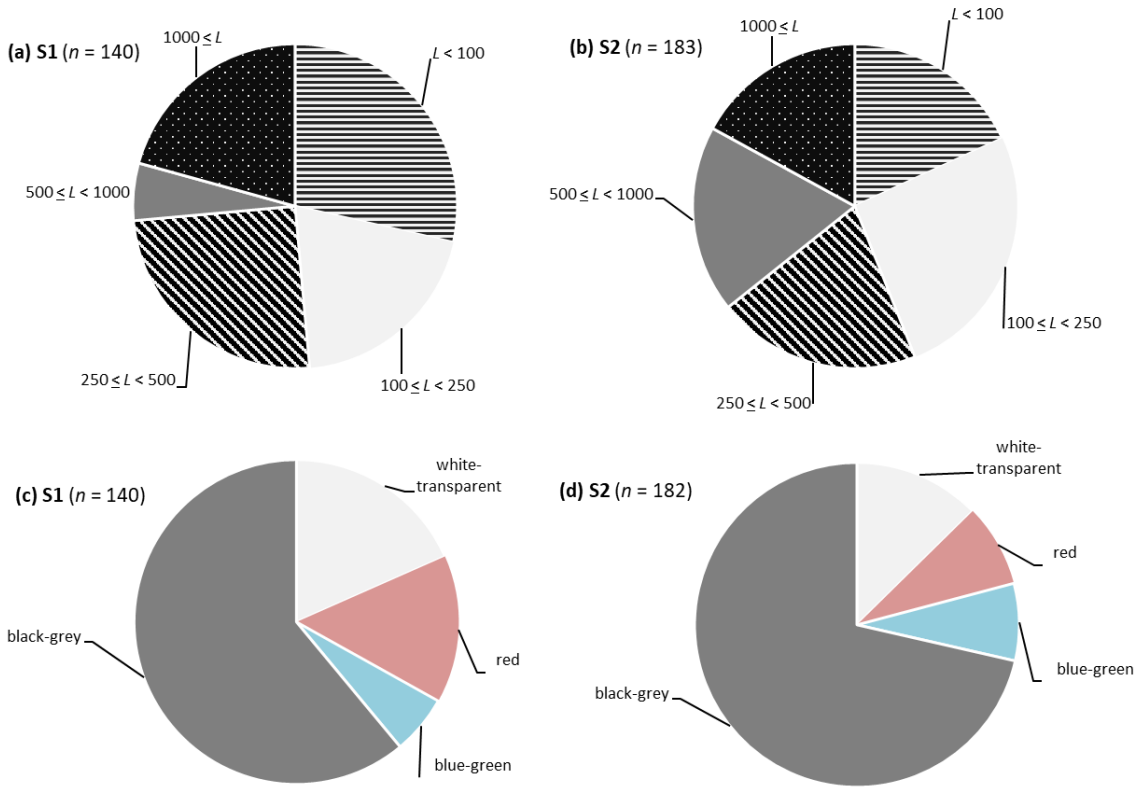

Figure 2: Size (in µm) and colour distribution of MPs at the two stations.

Imaging of selected samples by SEM, exemplified in Figure 3, revealed that most MP consisted of single straight, curved or coiled threads of 15 to 35 µm in diameter that were transversally round, many of which were smooth and clean. However, occasional samples consisted of multiple threads that were intertwined, entangled or bundled and that tended to exhibit greater degrees of mechanical and chemical weathering (pits, grooves, flaking). Some fibres appeared to be contaminated by extraneous solids, with EDX analysis confirming the presence of inorganic and organic geogenic material (e.g., Al, Ca, Na, Si) and residual salts arising from sample separation and preparation.

233

234

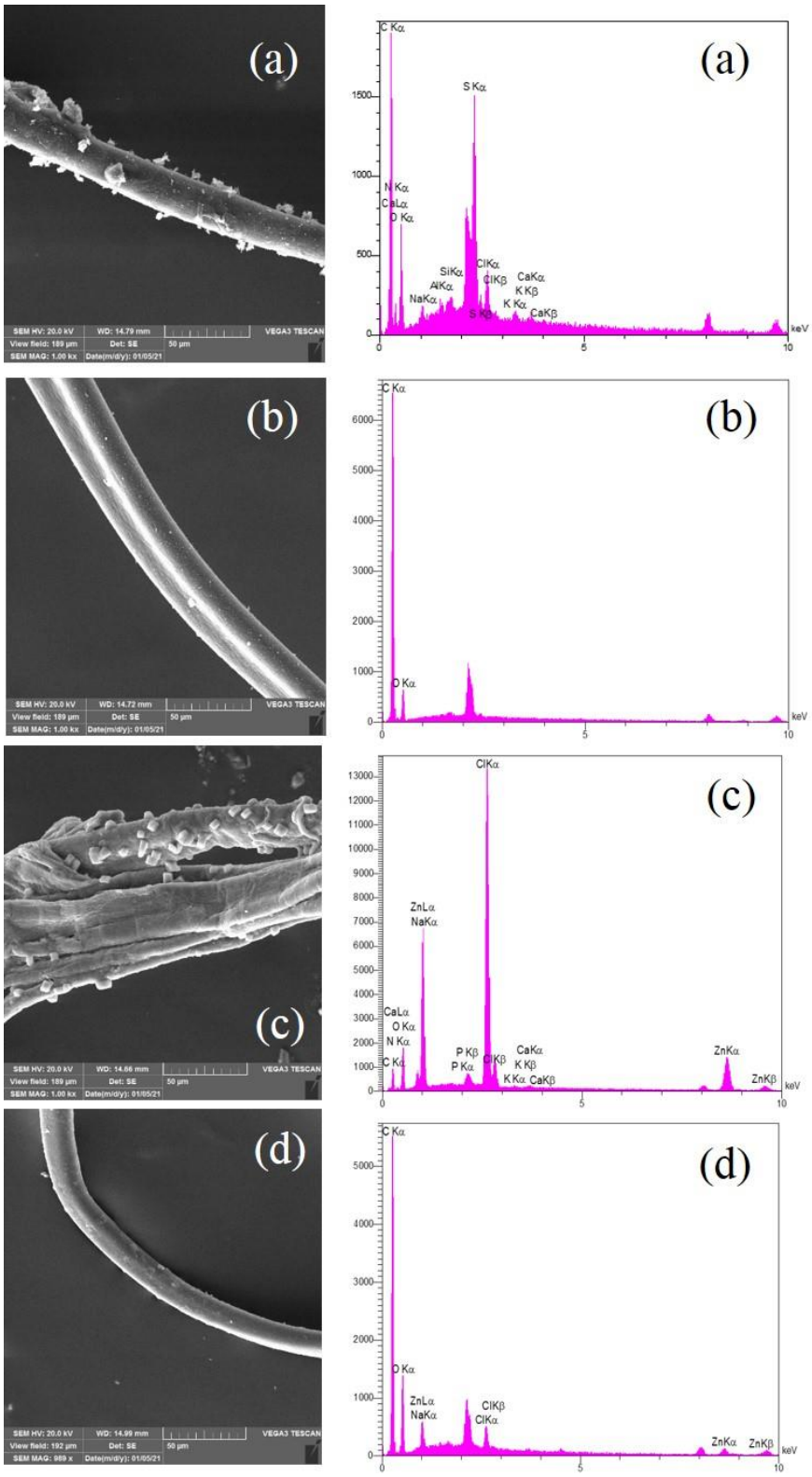
(a)
(b)
(c)
(d)
C Kα
S Kα
N Kα
CaLα
O Kα
SiKα
AlKα
NaKα
ClKα
ClKβ
CaKα
K Kβ
K Kα
CaKβ
ZnLα
NaKα
P Kβ
P Kα
ZnKα
ZnKβ
keV

235

Figure 3: SEM images and EDX spectra for four selected samples. (a) A blue PET fibre showing contamination by extraneous PM containing S, Na, Ca, K, Al and Si, (b) a red Nylon fibre, (c) intertwined white PET fibres with evidence of contamination by extraneous PM and residual $ZnCl_2$ arising from sample separation and (d) a blue PET fibre with evidence of contamination by NaCl.

4. Discussion

Despite a strong seasonality across the sampling period (and in particular, a significant drop in temperature from August to December), airborne concentrations of PM with a maximum aerodynamic diameter of 10 μm were rather constant at both stations in Ahvaz. The temporal distribution of MPs, however, was more heterogeneous, with no clear seasonal modification of the type, size or abundance at either station, and no clear difference in these characteristics between the two stations. The dominance of fibres and plastics mainly constructed of PET (a polyester), nylon (a polyamide) and polypropylene are consistent with the few previous studies that have actively sampled outdoor air and characterised suspended MPs (Dris et al., 2017; Liu et al., 2019a; Liu et al., 2019b; González-Pleiter et al., 2021) and confirm the ubiquity of such particulates in the atmosphere. However, the concentrations of MPs on a number basis that we observe (always < 0.02 m^{-3} and an overall median where MPs were detected of 0.0065 m^{-3}) are low compared with these studies.

Thus, Dris et al. (2017) observed concentrations of fibres in suburban Paris ranging from 0.3 to 1.5 m^{-3} (median 0.9 m^{-3}), although only one third of the fibres were plastic- (petroleum-) based, and in Asaluyeh County, Iran, Abbasi et al. (2019) found concentrations of MPs ranging from 0.3 to 1.1 m^{-3} (mean 1 m^{-3}). In different municipal districts of Shanghai, Liu et al. (2019a) obtained MP concentrations ranging from none detected to 4.2 m^{-3} (mean 1.4 m^{-3}), with higher concentrations than in Paris attributed to a greater population density and more intense industrial activities, despite a number of air cleaning activities conducted in the city. Liu and co-workers extended the study into the western Pacific Ocean and obtained concentrations

ranging from none detected to 1.4 m^{-3}, with a median of 0.01 m^{-3} (Liu et al., 2019b). One reason for the lower concentrations reported in the present study is that we based our sampling approach on a high volume EPA method for capturing PM10 (EPA, 1999). This employs an inlet cutoff equivalent to an aerodynamic diameter of 10 µm, or a diameter of a unit density sphere having the same terminal settling velocity as the particle in question, and captures particles that, in theory, have the greatest propensity to be inhaled through the human respiratory system. This approach may also explain why we did not detect other shapes of MP (e.g., spheres, granules or fragments) on the filters.

Fibrous MPs are likely to be generated from synthetic textiles and fabrics used in clothing, upholstered furnishings and carpets, industry and automobiles (Dris et al., 2017; Wright et al., 2020; Zhang et al., 2020), with the dominant polymer types identified in the present study (PET, polyamide, polypropylene) consistent with their importance in these sectors (Urdogan, 2012; Turner, 2019) and in indoor air (Dris et al., 2017). The proximity of the stations in Ahvaz to residential and industrial areas suggests that local sources of fibrous MPs might be important, with those fibres exhibiting little evidence of weathering presumably derived recently. However, the detection of fibrous MPs in locations remote from any anthropogenic sources, including the Alps, Pyrenees, Arctic and various protected areas of the US (Allen et al., 2019; Bergmann et al., 2019; Brahney et al., 2020), as well as above the planetary boundary layer (González-Pleiter et al., 2021), suggests that long-range transport with regional air masses may also be important. Transport of domestic, automotive, industrial and agricultural fibres over long distances, coupled with regular interactions with surface (ground) materials and features, may account for the mechanical and chemical weathering observed on many fibres sampled in the present study.

Results of our trajectory modelling using HYSPLIT are exemplified in Figure 4. Within the constraints and limitations of this approach (and mainly the assumption that MPs are carried in the same direction and with the same velocity as air itself and without deposition and re-entrainment), the results indicate the broad regions from which MP may have been transported into Ahvaz in the short-term. Thus, on most occasions considered, trajectories spread immediately to the north and northwest, with 90% frequencies extending to 300 to 600 km. Towards late autumn, however, a southerly component was sometimes observed with the highest frequencies located over the Persian Gulf. One of the fibres examined by SEM-EDX that was sampled when trajectories were southerly revealed the presence of Na and Cl without any other geogenic signature (Figure 3d), consistent with residual NaCl from a maritime source. Overall, the trajectories embrace a range of land uses, agricultural practices, industries, geomorphologies and demographics which may, at least partly, account for the heterogeneity of the fibrous MPs observed in Ahvaz in the present study.

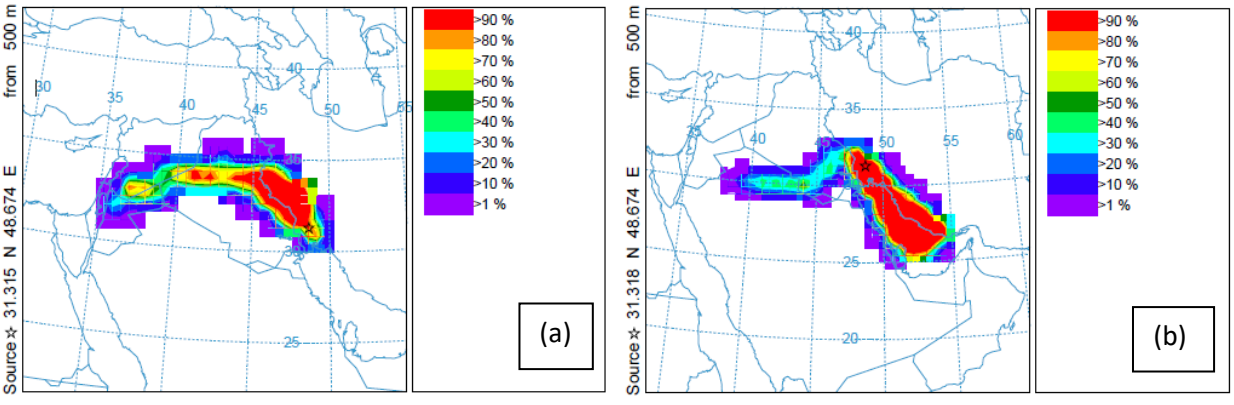

Figure 4: Twenty-four-hour back-trajectory frequency distributions calculated for Ahvaz (located with a star) on (a) 4/9/2019 and (b) 7/12/19.

Regarding human exposure, and assuming that on average 15 m^3 of air is inhaled daily and that ten hours per day are spent outdoors, our data suggest that up to about 0.1 fibrous MP whose

aerodynamic diameters, by operational definition, are less than 10 μm are consumed over a 24-hour period. This compares with the consumption of up to about 180 fibrous MP when exposed to indoor air containing 20 MP m^{-3} (determined by Dris et al., 2017) assuming that fourteen hours per day are spent inside. Although this comparison is subject to errors and uncertainties associated with the precise aerodynamic dimensions of the collection systems employed, the lower size limit of MP detection, the ability of the respiratory system to filter out fibres, and the habits of individuals and the conditions and styles of their homes, it is clear that MP exposure to the general public is far more important in the indoor setting than the outdoor environment. Nevertheless, the more general impacts of airborne and deposited fibrous MPs on terrestrial flora, fauna and ecosystems are largely unknown and require further study (He et al., 2020; Liu et al., 2020).

5. Conclusions

Airborne MPs collected with PM10 from urban and residential locations in Ahvaz over an extended, seasonal period, were fibrous in nature. However, abundance and characteristics displayed no clear temporal trends or differences between the two locations, with overall maximum and median concentrations of 0.017 and 0.0065 m^{-3}, respectively. Fibres were dominated by PET, polyamide and polypropylene, reflecting their use in synthetic textiles and fabrics, and displayed varying degrees of weathering and contamination by extraneous geogenic particles. The latter observation suggests both local and more distal origins of MPs, with HYSPLIT back trajectories indicating regional sources to the north and west of Ahvaz and a southerly, maritime source in late autumn. As components of PM10, further research is required into any possible impacts of fibrous MPs on human health and wildlife.

Acknowledgments

The authors are grateful for the logistic, technical and financial assistance from Shiraz and Ahvaz universities.

References

Abbasi, S., Keshavarzi, B., Moore, F., Turner, A., Kelly, F.J., Dominguez, A.O., Jaafarzadeh, N., 2019. Distribution and potential health impacts of microplastics and microrubbers in air and street dusts from Asaluyeh County, Iran. Environmental Pollution 244, 153–164.

Allen, S., Allen, D., Phoenix, V.R., Le Roux, G., Jimenez, P.D., Simonneau, A., Binet, S., Galop, D., 2019. Atmospheric transport and deposition of microplastics in a remote mountain catchment. Nature Geoscience 12, 339-344.

Allen, S., Allen, D., Moss, K., Le Roux, G., Phoenix, V.R., Sonke, J.E., 2020. Examination of the ocean as a source for atmospheric microplastics. PLoS ONE 15, e0232746.

Bergmann, M., Mützel, S., Primple, S., Tekman, M.B., Trachsel, J., Gerdts, G., 2019. White and wonderful? Microplastics prevail in snow from the Alps to the Arctic. Science Advances 5, eaax1157.

Brahney, J., Hallerud, M., Heim, E., Hahnenberger, M., Sukumaran, S., 2020. Plastic rain in protected areas of the United States. Science 368, 1257-1260.

Browne, M.A., Crump, P., Niven, S.J., Teuten, E., Tonkin, A., Galloway, T., Thompson, R., 2011. The physical impacts of microplastics on marine organisms: a review. Environmental Science and Technology 45, 9175–9179.

Buks, F., Kaupenjohann, M., 2020. Global concentrations of microplastics in soils – a review. Soil 6, 649-662.

Cai, L., Wang, J., Peng, J., Tan, Z., Zhan, Z. Tan, X., Chen, Q., 2017. Characteristic of microplastics in the atmospheric fallout from Dongguan city, China: preliminary research and first evidence. Environmental Science and Pollution Research DOI 10.1007/s11356-017-0116-x.

Constant, M., Ludwig, W., Kerhervé, P., Sola, J., Charrière, B., Sanchez-Vidal, A., Canals, M., Heussner, S., 2020. Microplastic fluxes in a large and a small Mediterranean river catchments: The Têt and the Rhône, Northwestern Mediterranean Sea. Science of the Total Environment 716, 136984.

Dris, R., Gasperi, J., Saad, M., Mirande, C., Tassin, B., 2016. Synthetic fibers in atmospheric fallout: a source of microplastics in the environment? Marine Pollution Bulletin 104, 290–293.

Dris, R., Gasperi, J., Mirande, C., Mandin, C., Guerrouache, M., Langlois, V., Tassin, B., 2017. A first overview of textile fibers, including microplastics, in indoor and outdoor environments. Environmental Pollution 221, 453-458.

EPA, 1999. Compendium Method IO-2.1. Sampling of ambient air for total suspended particulate matter (SPM) and PM10 using high volume (HV) sampler. Center for Environmental Research Information, U.S. Environmental Protection Agency, Cincinnati, Ohio.

Erdogan, U.H., 2012. Effect of pile fiber cross section shape on compression properties of polypropylene carpets. Journal of the Textile Institute 103, 1369-1375.

González-Pleiter, M., Edo, C., Aguilera, A., Viúdez-Moreiras, D., Pulido-Reyes, G., González-Toril, E., Osuna, S., de Diego-Castilla, G., Leganés, F., Fernández-Piñas, F., Rosal, R., 2021. Occurrence and transport of microplastics sampled within and above the planetary boundary layer. Science of the Total Environment 761, 143213.

385 Higado-Ruz, V., Gutow, L., Thompson, R.C., Thiel, M., 2012. Microplastics in the marine
386 environment: A review of the methods used for identification and quantification.
387 Environmental Science and Technology 46, 3060-3075.

388 He, D.H., Bristow, K., Filipovic, V., Lv, J.L., He, H.L., 2020. Microplastics in terrestrial
389 ecosystems: A scientometric analysis. Sustainability 12, 8739.

390 Li, J.Y., Liu, H.H., Chen, J.P., 2018. Microplastics in freshwater systems: A review on
391 occurrence, environmental effects, and methods for microplastics detection. Water Research
392 137, 362-374.

393 Liu, K., Wang, X., Fang, T., Xu, P., Zhu, L., Li, D., 2019a. Source and potential risk
394 assessment of suspended atmospheric microplastics in Shanghai. Science of the Total
395 Environment 675, 462–471.

396 Liu, K., Wu, T., Wang, X., Song, Z., Zong, C., Wei, N., Li, D., 2019b. Consistent transport of
397 terrestrial microplastics to the ocean through atmosphere. Environmental Science and
398 Technology 53, 10612-10619.

399 Liu, K., Wang, X.H., Song, Z.Y., Wei, N., Li, D.J., 2020. Terrestrial plants as a potential
400 temporary sink of atmospheric microplastics during transport. Science of the Total
401 Environment 742, 140523.

402 Roblin, B., Ryan, M., Vreugdenhil, A., Aherne, J., 2020. Ambient atmospheric deposition of
403 anthropogenic microfibers and microplastics on the western periphery of Europe (Ireland).
404 Environmental Science and Technology 54, 11100-11108.

405 Szewc, K., Graca, B., Dolega, A., 2021. Atmospheric deposition of microplastics in the
406 coastal zone: Characteristics and relationship with meteorological factors. Science of the
407 Total Environment 761, 143272.

Stanton, T., Johnson, M., Nathanail, P., MacNaughton, W., Gomes, R.L., 2019. Freshwater and airborne textile fibre populations are dominated by 'natural', not microplastic, fibres. Science of the Total Environment 666, 377-389.

Turner, A., 2019. Trace elements in laundry dryer lint: A proxy for household contamination and discharges to waste water. Science of the Total Environment 665, 568-573.

Wright, S.L., Ulke, J., Font, A., Chan, K.L.A., Kelly, F.J., 2020. Atmospheric microplastic deposition in an urban environment and an evaluation of transport. Environment International 136, 105411.

Zhang, Y., Kang, S., Allen, S., Allen, D., Gao, T., Sillanpää, M., 2020. Atmospheric microplastics: A review on current status and perspectives. Earth-Science Reviews 203, 103118.